Characterization of Micelles of Quaternary Ammonium Surfactants as Reaction Media I: Dodeclytrimethylammonium Bromide and Chloride

Barney L. Bales*,† and Raoul Zana‡

Department of Physics and Astronomy and the Center for Supramolecular Studies, California State University at Northridge, California 91330-8268, and Institut C. Sadron (ICS-ULP), 6 rue Boussingault, 67000 Strasbourg, France

Received: October 15, 2001; In Final Form: December 12, 2001

Time-resolved fluorescence quenching (TRFQ) and electron paramagnetic resonance (EPR) were employed to characterize micelles of dodecyltrimethylammonium bromide and chloride (DTAB and DTAC) as reaction media. For DTAB, the aggregation numbers, N, and the quenching rate constant of pyrene by hexadecylpyridinium chloride, k_q, were measured with TRFQ. Both these aggregation numbers for DTAB and those for DTAC taken from the literature depend only on the concentration of counterions in the aqueous phase, C_{aq}, whether these counterions are supplied by the surfactant alone or by surfactant plus added salt. Both surfactants conform to the power law $N = N^0(C_{aq}/\mathrm{cmc}_0)^\gamma$ where N^0 is the aggregation number at the critical micelle concentration in the absence of any additives (cmc_0). N^0 and γ differ for the two surfactants and vary with temperature in DTAB. EPR is employed to investigate the microviscosity and the hydration of the polar shell using a spin probe. The hydration is expressed by the nonempirical polarity parameter H, defined to be the ratio of molar concentration of OH dipoles in a solvent to that in water. For a solvent containing no other source of OH dipoles, H is the volume fraction occupied by water. This fraction decreases continuously with N from about 55% to 30% as the micelles grow from $N = 48$ to 73. Theoretical values of H are computed from a simple classical micelle model of a hydrocarbon core surrounded by a polar shell and compared with experiment. The model yields the number of water molecules per surfactant molecule, N_{H_2O}, which decreases continuously with N for DTA^+ micelles independent of the counterion. These results suggest that cationic micelles are dryer at all values of N than their twelve carbon anionic counterpart, sodium dodecyl sulfate (SDS); moreover, they lose waters of hydration faster as a function of N. The microviscosity of the polar shell, as deduced from the rotational correlation time of the nitroxide moiety of the spin probe, shows a modest increase with the aggregation number, comparable to that found in SDS. These viscosities are used to show that the quenching rate constant of pyrene by hexadecylpyridinium chloride in DTAB and of 1-methylpyrene by tetradecylpyridinium chloride in DTAC follow a common Stokes−Einstein−Smolukhovsky equation with a quenching probability of $P = 0.4$. This is so whether the micelle aggregation number, the temperature, or the counterion is changed. The microviscosity of the polar shell of DTAB shows a normal liquid-state temperature activation energy that is comparable to that found in ethanol−water mixtures. DTAB and DTAC are the same medium with respect to their hydration and the collision rate of guest molecules. By employing different combinations of surfactant and salt concentrations leading to the same values of N, a value for the degree of counterion dissociation for DTAB at 25 °C was derived from both the TRFQ $\alpha = 0.23 \pm 0.03$ and EPR $\alpha = 0.257 \pm 0.010$ which are in good agreement with each other and with literature values. From EPR, at 10.1 °C, $\alpha = 0.190 \pm 0.008$ and at 45 °C, $\alpha = 0.273 \pm 0.011$. For DTAC, $\alpha = 0.365 \pm 0.008$, derived from EPR, is also in good agreement with literature values. With respect to the fraction of counterion concentrations associated with the micelle, DTAB and DTAC differ substantially.

Introduction

A considerable amount of basic research has attempted to characterize micelles as reaction media.[1−4] As a reaction medium, a micelle presents a highly restricted volume through which guest molecules may diffuse, collide, and react. To characterize a micelle as a medium, it is necessary to determine its size, level of hydration, microviscosity, and degree of counterion dissociation. Progress in achieving a deep understanding of these physicochemical properties of micelles has been limited[2] because an understanding of both the structural and the dynamic properties must be achieved simultaneously. There does not exist a single technique capable of supplying all of these types of information unambiguously; thus, there is a need to combine techniques in order to increase the information and thereby decrease the uncertainties.

In this work, we interpret the results of time-resolved fluorescence quenching (TRFQ) and electron paramagnetic resonance (EPR) in the framework of a classical micelle model as a spherical hydrocarbon core surrounded by a polar shell. The theoretical value of the hydration of the micelle is calculated from a simple geometrical model and compared with the

* To whom correspondence should be addressed. E-mail: barney.bales@email.csun.edu.

† Department of Physics and Astronomy and the Center for Supramolecular Studies, California State University at Northridge.

‡ Institut C. Sadron (ICS-ULP).

10.1021/jp013813y CCC: $22.00
Published on Web 02/02/2002

TABLE 1: Nomenclature and Abbreviations

$C_{16}PC$, $C_{14}PC$	hexadecyl, tetradecylpyridinium chloride quenchers
Py, 1-MePy	fluorophores pyrene, 1-methylpyrene
16DSE	nitroxide spin-probe 16-doxylstearic acid ester
SDS, LiDS	sodium, lithium dodecyl sulfate
DTAB, DTAC	dodecyltrimethylammonium bromide, chloride
EPR	electron paramagnetic resonance
LS	light scattering
SANS	small-angle neutron scattering
TRFQ	time-resolved fluorescence quenching
α	ionization degree of micelles
η	viscosity
A_+	hyperfine spacing between the low-and center-field EPR lines
C_{ad}	concentration of added common counterion in the form of salt
C_{aq}	concentration of the counterion in the aqueous phase; $[Br^-]_{aq}$ or $[Cl^-]_{aq}$
cmc, cmc_0	critical micelle concentration in general, and in the absence of salt
[Q]	quencher concentration in the sample
C_Q	quencher concentration in the polar shell
V	molar volume of the dry surfactant
H	nonempirical polarity index[28]; volume fraction occupied by water
k_D	bimolecular collision rate between the fluorophore and the quencher
k_q	first order quenching rate constant of the fluorophore by one quencher
P	quenching probability of the fluorophore upon collision with the quencher
$\bar{n}$	average number of quenchers per micelle
N, N^0	aggregation number in general, and at the cmc_0
N_{H_2O}	number of water molecules in the shell per surfactant molecule
N_0	Avogadro's number
N_c	number of carbons in the alkyl chain; $N_c = 12$
N_{wet}, $N_{wet}{}^0$	number of methylene groups residing in the polar shell; and at the cmc_0
R_h	hydrodynamic radius of the spin probe
R	the gas constant
R_c	radius of the hydrocarbon core
R_m	radius of the micelle
S_f	surfactant concentration in monomer form
S_t	total surfactant concentration
$F(S_t)$	excluded volume factor

experimental results derived from EPR. The viscosity of the polar shell is deduced from measurements of the rotational correlation time of a spin probe as a function of the micelle composition or the temperature. These viscosities are used to show that the quenching rate constants of pyrene (Py) by hexadecylpyridinium chloride ($C_{16}PC$) and by 1-methylpyrene (1-MePy) by tetradecylpyridinium chloride ($C_{14}PC$), measured by TRFQ, follow a classical hydrodynamic description.

Parallel to the development of this line of physical characterization of micelles as reaction media,[3,5] an elegant, complementary chemical approach is emerging due to the work of Romsted and co-workers, ref 4 and the references therein. Their approach uses chemical trapping of weakly basic nucleophiles, including water, at the interface of micelles by arenediazonium salts. Information about micelle hydration[4] and degree of counterion dissociation[6] is available in some cases. Their approach, based on what appears to be the reasonable assumption that the chemical yields of certain reactions are monotonic in the local concentrations of the reactants,[6−9] does not require knowledge about the aggregation numbers. Chemical trapping has not yet been applied to DTAB or DTAC,[8] so a direct comparison is not yet possible; however, it will be very interesting to see to what extent the two approaches can be combined to understand micelles as reaction media.

This work, which is a continuation of investigations in sodium dodecyl sulfate[5] (SDS) and mixed micelles of SDS and a sugar-based nonionic surfactant,[3] is prerequisite to the study of quaternary ammonium dimeric and oligomeric surfactants in aqueous solution.

Table 1 is a glossary of the most frequently used symbols and abbreviations in this work.

Methods

TRFQ. Fluorescence decay data were accumulated using the time-correlated single-photon counting technique[10] using procedures that are standard.[11−15] In these experiments, Py was used as the fluorescence probe and $C_{16}PC$ as the quencher. Samples were prepared without quencher or with approximately one quencher per micelle and were degassed by three freeze−pump−thaw cycles. DTAB, DTAC, Py, and $C_{16}PC$ were purified as previously described[16] and MilliQ water was the solvent. The temperature was controlled by a circulating water bath and was measured with a thermocouple. The decay curves were fit to the Infelta−Tachiya equation,[13,17] yielding, as expected for Py and $C_{16}PC$, parameters consistent with negligible inter micelle migration of the quencher or probe during the lifetime of the Py fluorescence. The fits yield the average number of quenchers per micelle, $\bar{n}$, and the rate of quenching due to one quencher, k_q. The assumptions involved in this analysis have been exhaustively discussed in the literature to which the reader is referred.[13,17,18]

From $\bar{n}$, the average aggregation number, N, may be computed as follows

$$N = \frac{\bar{n}(S_t - S_f)}{[Q]} \qquad (1)$$

where S_t and $[Q]$ are the concentrations (mol L^{-1} of solution) of the surfactant and quencher, respectively. S_f is the molar concentration of the surfactant in monomer form which may be computed using eq 5 of ref 19 derived from the work of Sasaki et al.[20] and Hall,[21] as follows

$$\log(S_f) = (2 - \alpha)\log(cmc_0) - (1 - \alpha)\log(C_{aq}) \qquad (2)$$

where α is the degree of counterion dissociation, cmc_0 is the critical micelle concentration (cmc, in mol L^{-1}) in the absence of additives, and C_{aq} is the molar concentration of counterions in the aqueous phase, given by eq 21 below. See ref 19 and references therein for a discussion of the assumptions leading to eq 2. At low values of C_{aq}, the values of S_f given by eq 2 are sensitive to the value of cmc_0 but are rather insensitive to the value of α.

EPR. Experimental details for the EPR measurements are identical to those described recently;[3] essential details are summarized. Mother solutions of the surfactants prepared at concentrations $S_t \approx 350$ mM containing the spin probe 16-doxylstearic acid methyl ester (16DSE) with a surfactant-to-probe ratio of 500:1 were prepared in MilliQ water. Solutions with various combinations of surfactant and salt were prepared from the mother solution by weight and their concentrations calculated from their known densities.[22,23] Computer fits of the EPR spectra yield the line positions and line heights to high precision.[24]

Rotational correlation times are computed from the line height ratios using standard formulas[25] and are corrected for inhomogeneous line broadening.[26] Two independent values of the rotational correlation time result,[25] τ_B and τ_C. Isotropic reorientation of the nitroxide moiety yields $\tau_B = \tau_C$, thus the

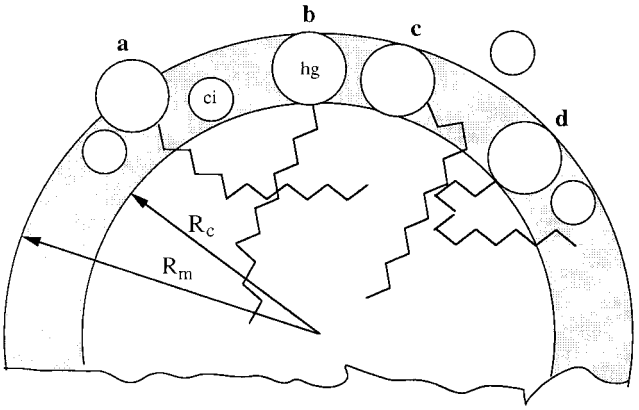

Figure 1. Schematic of the polar shell model, with hydrocarbon core of radius R_c and micelle radius R_m. The circles labeled hg and ci represent the headgroups and the counterions, respectively. Unoccupied volume in the polar shell, the shaded region, is filled with water. Hydrocarbon from the surfactant in arrangement ***b*** is entirely within the core while in arrangements ***a***, ***c***, and ***d***, it partially occupies the polar shell. In ***a*** and ***c***, methylene groups occupy the polar shell, whereas in ***d***, a methyl group enters first, perhaps followed by methlene groups.

departure of the ratio τ_B/τ_C from unity is a measure of the anisotropy of the motion.[27] The effective rotational correlation time is defined by[27]

$$\tau_{\text{measured}} = \sqrt{\tau_B \tau_C} \tag{3}$$

From the EPR line positions, the hyperfine spacing between the center- and low-field lines, A_+, is computed. Mukerjee et al.[28] introduced a nonempirical polarity scale, H, defined to be the ratio of molar concentration of OH dipoles in a solvent or solvent mixture to that in water. The scale is nonempirical because only the molecular structure of the components of the mixture and the density are required to calculate H. For solvent mixtures with no other source of OH dipoles than water, H is equal to the volume fraction occupied by water. For the spin probe 16DSE, A_+, given in Gauss, has been shown[29] to vary linearly with H as follows

$$A_+ = 14.309 + 1.418\,H \tag{4}$$

See refs 3, 5, 28−31, and references therein for a thorough discussion of the suitability of the use of the solvatochromic properties of nitroxide free radicals to study lipid assemblies such as micelles, the theoretical basis[30] for the variation of A_+ with H, and the methods[5,29] to obtain calibration curves such as eq 4. In particular, Mukerjee et al.[28] showed that a wide range of different solvents and solvent mixtures lead to the same value of A_+ for a given value of H. We have discussed[31] the fact that the presence of high concentrations of ions in the polar shell does not affect the use of eq 1.

Theory

Hydration Model. We employ a simple model based upon a classical picture[32−41] of a nearly spherical micelle having a hydrocarbon core with very little water penetration[42] surrounded by a polar shell. The polar shell contains the $N^+(CH_3)_3$ headgroups, a fraction, $(1 - \alpha)$, of the counterions (Cl^- or Br^-), water, and a number, N_{wet}, of the methylene groups from the hydrocarbon tail. The thickness of the polar shell is taken to be constant as a function of N at constant temperature. See Figure 1 for a schematic view of the core−shell model.

Thus, the geometry of the micelle is characterized by the radius of the hydrocarbon core, R_c, and the radius of the micelle, R_m. The volume of the core is taken to be NV_{tail}, where V_{tail} is the volume (Å^3) occupied by the saturated hydrocarbon chain, embedded in the core, calculated according to Tanford (p 52 of ref 43) as

$$V_{\text{tail}} = 27.4 + 26.9\,(N_c - N_{\text{wet}}) \tag{5}$$

where N_c is the number of carbon atoms per alkyl chain. Thus, the core radius is found from

$$NV_{\text{tail}} = \frac{4\pi}{3} R_c^{\,3} \tag{6}$$

Assigning a thickness to the polar shell $R_m - R_c$ yields the radius of the micelle from which its volume may be computed

$$V_{\text{micelle}} = \frac{4\pi}{3} R_m^{\,3} \tag{7}$$

and the volume of the polar shell

$$V_{\text{shell}} = \frac{4\pi}{3}(R_m^{\,3} - R_c^{\,3}) \tag{8}$$

Previously, for SDS,[5] we assumed that the entire hydrocarbon chain was embedded in the core in keeping with adopting the simplest approach; however, here, we find it necessary to assume that $N_{\text{wet}} > 0$ reminiscent of the models used in the interpretation of small-angle neutron scattering(SANS) data.[32,36−40,44] See Figure 1 for several schematic arrangements that place surfactant hydrocarbon in the polar shell. The most satisfactory approach would be to determine N_{wet} from some other technique, for example, SANS; however, there is no agreement in the literature. For example, for DTAB, Hayter and Penfold[32] find N_{wet} to be approximately zero near $N = 57$ growing to about $N_{\text{wet}} = 2.4$ near $N = 82$, whereas Berr et al.[40] assumed a constant value of $N_{\text{wet}} = 4$ for all values of N. To avoid adjusting the value of N_{wet} at every value of N, effectively introducing many parameters, we assume that it is a slowly varying function of the aggregation number and retain the first two terms of its Taylor series expansion

$$N_{\text{wet}} \approx N_{\text{wet}}{}^0 + \frac{\partial N_{\text{wet}}}{\partial N}(N - N^0) \tag{9}$$

The volumes (Å^3) of the headgroup, counterion, methylene group, and water are denoted by V_{hg}, V_{ci}, V_{CH2}, and V_{H_2O}, respectively. The volume inaccessible to water per surfactant molecule, V_{dry}, is taken to be the total volume of the headgroups, the counterions, and the methylene groups as follows

$$V_{\text{dry}} = [V_{\text{hg}} + (1 - \alpha)V_{\text{ci}} + N_{\text{wet}}V_{\text{CH}_2}] = [V_{\text{dry}}{}^0 + N_{\text{wet}}V_{\text{CH}_2}] \tag{10}$$

where $V_{\text{dry}}{}^0 = V_{\text{hg}} + (1 - \alpha)V_{\text{ci}}$ is the (constant) volume inaccessible to water due to the headgroup and the counterions.

We find the volume of water in the polar shell by subtracting the volume inaccessible to water from the volume of the polar shell and from this compute the volume fraction occupied by water to be

$$H = (V_{\text{shell}} - NV_{\text{dry}})/V_{\text{shell}} \tag{11}$$

Let N_{H_2O} denote the average number of water molecules per surfactant residing in the polar shell. Thus, $V_{H_2O}N_{H_2O}N$ is

TABLE 2: Volumes used in the Analysis (25 °C)

symbol	group	volume, Å^3
V_{hg}	$N^+(CH_3)_3$	106[a]
V_{H_2O}	H_2O	30[b]
V_{ci}	Cl^-	28.9[b]
V_{ci}	Br^-	39.3[b]
V_{CH_2}	CH_2	26.9[c]
V_{CH_3}	CH_3	54.3[c]
V_{dry}^0	$N^+(CH_3)_3$ & Cl^-	124[d]
V_{dry}^0	$N^+(CH_3)_3$ & Br^-	135[e]

[a] The average from refs 32 and 45. [b] Ref 32. [c] Ref 43. [d] $V_{dry}^0 = V_{hg} + (1 - \alpha)V_{ci}$ using $\alpha = 0.365$. [e] or $\alpha = 0.257$.

the volume of the water in the shell, yielding a volume fraction of

$$H = N\, V_{H_2O} N_{H_2O}/V_{shell} \tag{12}$$

Combining eqs 11 and 12, yields

$$N_{H_2O} = \frac{V_{shell} - NV_{dry}}{NV_{H_2O}} \tag{13}$$

The values of the various volumes used in the calculations are given in Table 2. The values for V_{ci} are those that have been used[32] in the analysis of SANS data. The method of addition of partial molal volumes[45] gives systematically higher values for V_{ci} for both counterions, but the difference between V_{ci} for Cl^- and Br^- is similar, so the relative results between the two surfactants DTAB and DTAC are the same using either set. The final two rows of Table 2 give the values of V_{dry}^0 for the two surfactants. The absolute uncertainties in these volumes is about ±6%; however, their relative values are estimated to be correct to about ±2%.

Microviscosity from EPR Measurements of the Rotational Correlation Time. The microviscosity of the environment of a spin probe may be estimated utilizing the Debye−Stokes−Einstein equation[46]

$$\tau_{relative} = 4\pi\eta R_h^3/3kT \tag{14}$$

where η is the shear viscosity of the solvent, k the Boltzmann constant, T the absolute temperature, and R_h the hydrodynamic radius of the molecule which was found[3] to be $R_h = 3.75$ Å for the doxyl group of 16DSE. The subscript *relative* refers to reorientation of the spin probe relative to a liquid at rest. A procedure to apply the technique to a micelle was described in ref 47 which may be consulted for details on the background, assumptions, and procedures.

To estimate the microviscosity from rotational correlation times measured in the laboratory frame of reference, $\tau_{measured}$, the overall motion of the doxyl group is modeled as a reorientation relative to the micelle as a unit with rotational correlation time $\tau_{relative}$ and an isotropic reorientation of the micelle as a whole of $\tau_{micelle}$. These reorientations are assumed to be independent, so

$$\frac{1}{\tau_{measured}} = \frac{1}{\tau_{relative}} + \frac{1}{\tau_{micelle}} \tag{15}$$

$\tau_{micelle}$ is computed from the Debye−Stokes−Einstein equation written as follows

$$\tau_{micelle} = V_{micelle} \cdot \frac{\eta_w}{kT} \tag{16}$$

where $V_{micelle}$ is found from eq 7 and η_w is the viscosity of pure water.[48]

Hydrodynamic Description of Fluorescence Quenching in Micelles. A hydrodynamic theory of the collision rate between molecules in micelles was recently presented.[3] The fundamental hypothesis is that molecules that are sparingly soluble in water, and can therefore be concluded to be solubilized by the micelle, diffuse according to the Stokes−Einstein equation throughout the volume of the polar shell. The bimolecular collision rate between the probe and the quencher in liquids is based upon combining the Smolukhovsky and the Stokes−Einstein equations to yield the well-known expression[49] for the diffusional collision rate constant

$$k_D = \frac{8RT}{3000\eta} \tag{17}$$

where $R = 8.31$ J/°K is the gas constant and η has unit Poise. k_D has units L mol^{-1} s^{-1}. The rate constant k_q is proportional to the concentration of the quencher in the polar shell, C_Q

$$k_q = C_Q P k_D \tag{18}$$

where P is the probability that quenching occurs upon collision. Because k_q is the quenching rate due to one quencher, then C_Q is the molar concentration of one molecule in the volume V_{shell} thus

$$C_Q = \frac{10^{27}}{N_0 V_{shell}} \tag{19}$$

where N_0 is Avogadro's number. The factor 10^{27} converts the volume V_{shell} from Å^3 to liters.

Combining eqs 17−18

$$k_q = C_Q P \frac{8RT}{3000\eta} \tag{20}$$

Degree of Counterion Dissociation. Recently,[50] a definition of the degree of counterion dissociation based on the micelle aggregation number was proposed and demonstrated. The fundamental hypothesis is that N is uniquely given by the concentration of counterions in the aqueous pseudophase, C_{aq}, which, according to the conventional pseudophase ion exchange mass balance relationship[51,52] as modified by Soldi et al.[4] is given by

$$C_{aq} = F(S_t)\{\alpha S_t + (1 - \alpha)S_f + C_{ad}\} \tag{21}$$

where S_t, S_f, and C_{ad} are the molar concentrations of total surfactant, surfactant in monomer form, and added common counterion in the form of salt, respectively. The factor within the brackets would give the concentration of counterions in the aqueous phase if that phase occupied the entire sample; however, at higher surfactant concentrations the excluded volume effect becomes important.[4] Following Soldi et al.,[4] we correct for this excluded volume effect by including the factor $F(S_t)$

$$F(S_t) = \frac{1}{1 - VS_t} \tag{22}$$

where V is the molar volume of the anhydrous surfactant in L mol^{-1} assuming that the density of the surfactant is approximately 1.0 g/mL.[4] $V = 0.308$ L mol^{-1} for DTAB and 0.264 L mol^{-1} for DTAC.

A value of α is measured by preparing two samples yielding the same value of the aggregation number, but with different values of S_t and C_{ad}. For these two samples the hypothesis asserts that the value of C_{aq} is the same as follows

$$F(S_t)\{\alpha S_t + [1-\alpha]S_f + C_{ad}\} = F(S_t')\{\alpha S_t' + [1-\alpha]S_f' + C_{ad}'\} \quad (23)$$

As previously discussed,[50] the terms involving S_f and S_f' cancel in eq 23, thus for an equivalent value of N, we have

$$F(S_t)\{\alpha S_t + C_{ad}\} = F(S_t')\{\alpha S_t' + C_{ad}'\} \quad (24)$$

A rearrangement of eq 24 yields the value of α

$$\alpha = \frac{F(S_t)C_{ad} - F(S_t')C_{ad}'}{F(S_t')S_t' - F(S_t)S_t} \quad (25)$$

Any property that varies monotonically with N could, in principle, be used to determine α. In principle, α could vary with C_{aq}; however, we previously showed that α is constant for SDS up to [SDS] = 600 mM.[50] This is in accord with theory[53] and is a reasonable assumption for the surfactant concentrations considered here, 350 mM or less. Thus, rather than computing α for each pair of samples, eq 25, a simpler approach is to require that all values of the measured property fall on a common curve when plotted versus the variable $F(S_t)\{\alpha S_t + C_{ad}\}$ as shown by eq 24. The procedure to determine α is illustrated in Figure 2 where the ordinate corresponds to any quantity that is monotonic in N. The property could either increase or decrease; Figure 2 supposes a property that increases. Solid circles correspond to data taken using a low, constant surfactant concentration while varying the salt concentration. The open circles are derived from salt-free samples. Many other combinations of salt and surfactant concentrations could be used. Figure 2b−2d shows the progression in which α is varied in the quantity $F(S_t)\{\alpha S_t + C_{ad}\}$ in search of a common curve. The solid lines in Figure 2b−2d are the least-squares fits to all data, both solid and open circles, using a trial function. The best value of α is found by finding the minimum least-squares deviations from the trial function. In the hypothetical case of Figure 2, the best value of α is α = 0.3. Such minima are easily found using a spread sheet having curve fitting capabilities. It is important to note that the value of N corresponding to the data is not needed. Note that the range of the abscissa is different in Figure 2a−2d.

Variation of N with C_{aq}. In 1995, it was recognized[19] that, for SDS micelles, the aggregation number shows a power law dependence on C_{aq} as follows[19]

$$N = N^0(C_{aq}/\mathrm{cmc}_0)^{\gamma} \quad (26)$$

{In earlier papers,[5,19,24,29] eq 26 was written $N = \kappa_2 C_{aq}\gamma$; eq 26 results by defining $N^0 = \kappa_2(\mathrm{cmc}_0)^{\gamma}$}. Since 1995,[19] eq 26 has been found to be valid for 7 other surfactants as follows: the sodium alkyl sulfates with chain lengths 8−14,[54,55] lithium dodecyl sulfate,[31] and cetyltrimethylammonium chloride and acetate.[56] In this work, we find that eq 26 also describes the aggregation numbers for DTAB and DTAC. Equation 26 is likely to describe many micelles; in fact, already in the 1950s, empirical equations of the same form as eq 26 were proposed where cmc + C_{ad} was the independent variable rather than C_{aq}, as is presently formulated. For work near the cmc, there is no difference between these two variables. See, for example, refs 57 and 58.

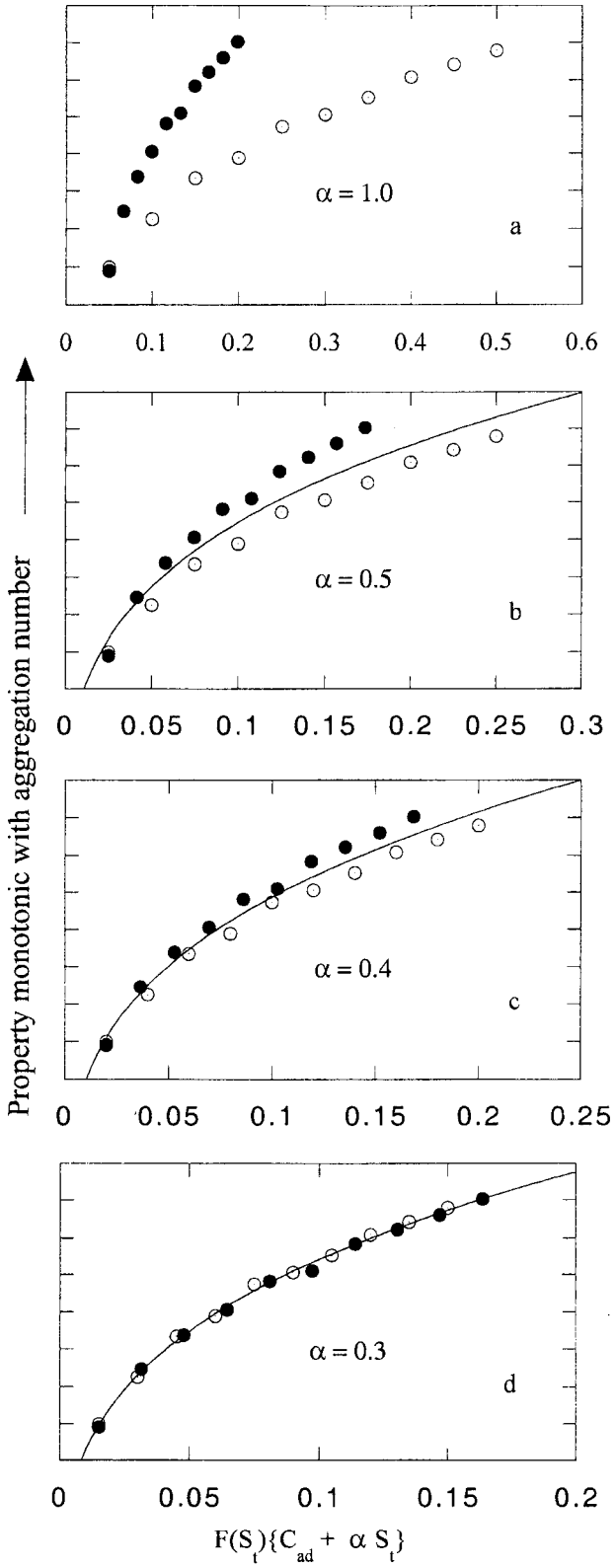

Figure 2. Schematic implementation of eq 24 to determine α by finding a common curve for any property that varies monotonically with the aggregation number. Property could increase or decrease with N; in this schematic it is assumed to increase. Solid circles correspond to data taken by adding salt to a low, constant surfactant concentration; open circles are derived from salt-free samples. Figure 2b−d show the progression in which α is varied in search of a common curve. Solid lines in 2b−2d are the least-squares fits to all data, both solid and open circles, using a trial function. Minimizing the mean square deviations from this line defines the best fit value of α; α = 0.3 in this hypothetical case. Note: the range of the abscissa is different in a−d.

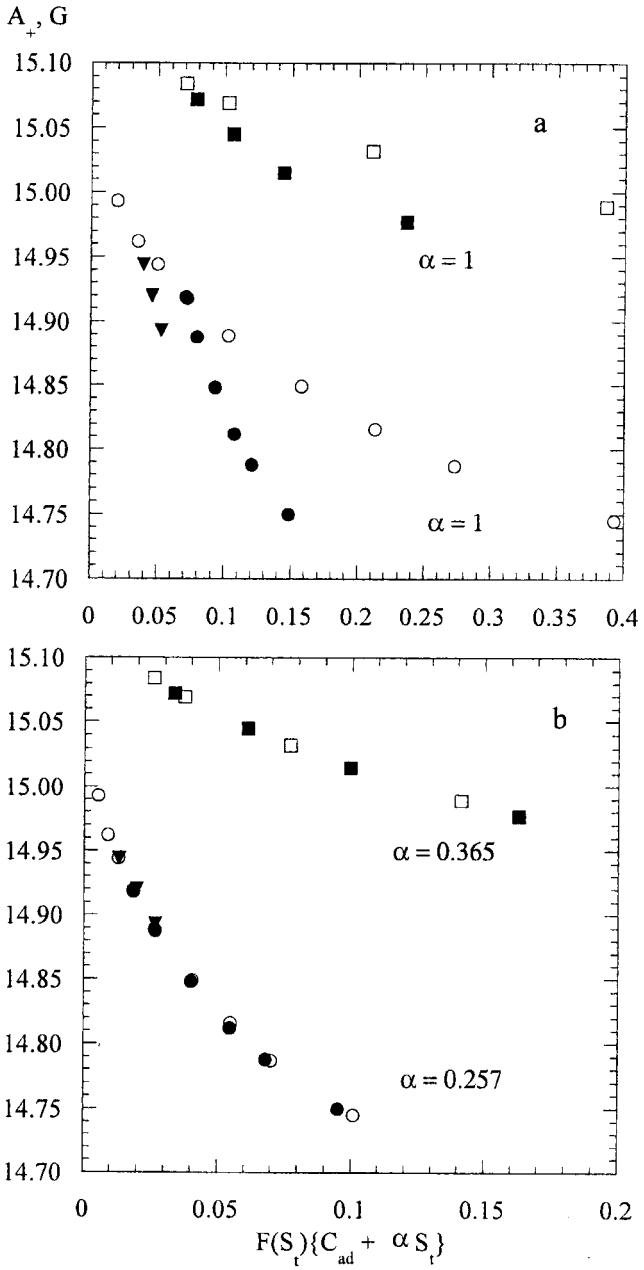

Figure 3. Hyperfine spacing A_+ versus $F(S_t)\{\alpha S_t + C_{ad}\}$ (a) $\alpha = 1$ for DTAB and $\alpha = 1$ for DTAC; (b) best fit values of $\alpha = 0.257$ for DTAB and $\alpha = 0.365$ for DTAC. Open symbols salt-free and filled symbols salt-added. [DTAB] = 20−350 mM, [NaBr] = 0, ○; [DTAB] = 70 mM, [NaBr] = 0−75 mM, ●; [DTAB] = 35 mM, [NaBr] = 0−17.6 mM, ▼; [DTAC] = 70−350 mM, [NaCl] = 0, □; [DTAC] = 70 mM, [NaCl] = 0−72 mM and, [DTAC] = 118 mM, [NaCl] = 0−112 mM, ■. T = 25 °C.

Results

Values of α from EPR. Three-line narrow EPR spectra of 16DSE typical of nitroxide free radicals undergoing approximately isotropic motion in the motional narrowing region were observed for all samples. See, for example, Figure 1(a) of ref 5. Figure 3a shows the variation of the hyperfine spacing A_+, with $F(S_t)\{S_t + C_{ad}\}$ for DTAB and DTAC. For open symbols, S_t is varied in the absence of salt and for closed, salt is added. Each point is the mean value of measurements from five spectra; the standard deviations are smaller than the size of the symbols. In a repeat of the DTAB experiment (data not shown) we found, as before,[50] that the reproducibility in the measurements of A_+ on a single sample is superior to the reproducibility in sample preparation. The former is typically 1 mG, whereas the latter averages about 4 mG in samples presumably prepared identically. On the scale of Figure 3, 4 mG is about the size of the symbols. Following the scheme of Figure 2, the value of α was varied by trial and error until a common curve was achieved for each surfactant. Figure 3b shows these common curves with $\alpha = 0.257$ for DTAB and $\alpha = 0.365$ for DTAC. The best common curves were judged by plotting the mean squared deviation of the data from a quadratic trial function. Such a plot for DTAB is shown in Figure 4 Similar measurements for DTAB at 10 and 45 °C yield values of $\alpha = 0.190$ and 0.273, respectively. The values of α determined on the basis of eq 24 are given in Table 3 which includes some literature values. See the Appendix for a discussion of the uncertainties in values of α derived from eq 24 using EPR.

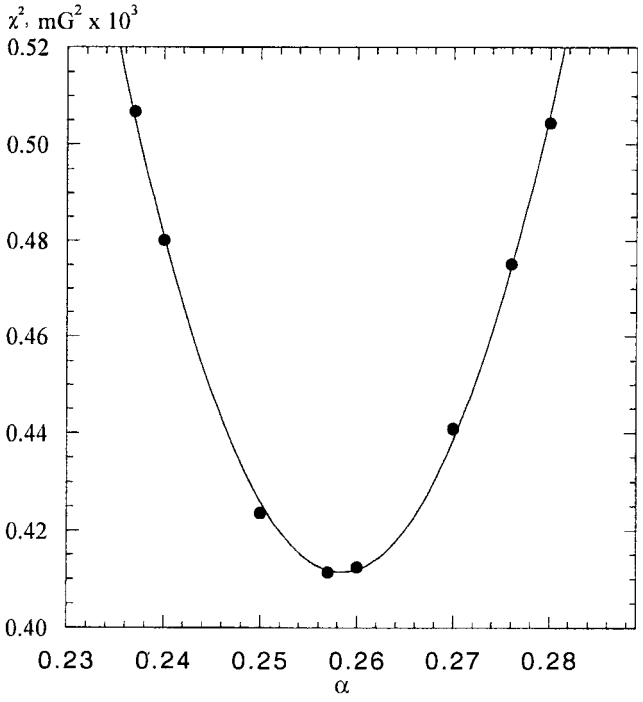

Figure 4. Mean square deviations, χ^2, of the values of A_+ from a quadratic trial function for DTAB as a function of α. $T = 25$ °C.

TABLE 3: Values of α (DTAB and DTAC)

	T, °C	α	technique	ref
DTAB	10.1	0.190 ± 0.008	eq 24 EPR	this work
	10	0.23	specific ion electrode	66
	25.0	0.257 ± 0.010	eq 24 EPR	this work
	25.0	0.22 ± 0.03	eq 24 TRFQ	this work
	25.0	0.25	specific ion electrode	66
		0.23	specific ion electrode	67
	25.0	0.26	conductivity slope	78
	25.0	0.27 ± 0.05(2)[a]	SANS	32,38
	25.0	0.20 ± 0.03(4)[a]	LS	58,79
	25.0	0.35 ± 0.11(3)[a]	cmc versus C_{ad}	80,81
	25.0	0.38	cmc versus C_{ad}	65
	25.0	0.23	specific ion electrode	65
	45.0	0.273 ± 0.011	eq 24 EPR	this work
	45	0.32	specific ion electrode	66
DTAC	25	0.365 ± 0.008	eq 24 EPR	this work
		0.34	conductivity slope	78
		0.32	SANS	32
		0.39	cmc versus C_{ad}	65
		0.42	specific ion electrode	65
		0.37 ± 0.05(4)[a]	cmc versus C_{ad}	61,80,81

[a] Mean values and standard deviations from unweighted fits to the number of values given in parentheses.

TABLE 4: Aggregation Numbers of DTAB

[DTAB], mM	[NaBr], mM	$[DTAB]_f$, mM[a]	$[Br^-]_{aq}$, mM[b]	$F(S_t)$[c]	*T*, °C	*N*
100	0	8.50	28.2	1.03	10.1	71.4 ± 1.6
200	0	5.50	46.5	1.07	10.1	79.6 ± 1.6
350	0	3.80	78.9	1.12	10.1	84.4 ± 1.7
100	0	8.50	32.6	1.03	25.0	58.2 ± 1.2
200	0	5.50	58.4	1.07	25.0	67.7 ± 1.3
350	0	3.80	102	1.12	25.0	72.4 ± 1.4
70.0	0	9.90	25.8	1.02	25.0	60.8 ± 1.3
70.0	8.04	8.50	32.7	1.02	25.0	63.0 ± 1.3
70.0	35.5	5.50	58.5	1.02	25.0	67.8 ± 1.4
70.0	74.4	3.80	97.0	1.02	25.0	72.2 ± 1.5
100	0	8.50	35.6	1.03	45.0	45.0 ± 1.9
200	0	5.50	63.3	1.07	45.0	50.1 ± 2.0
350	0	3.80	111	1.12	45.0	58.1 ± 2.3

[a] Equation 2 using the values of cmc_0 in Table 5 and α from EPR, Table 3. [b] Equation 21. [c] Equation 22.

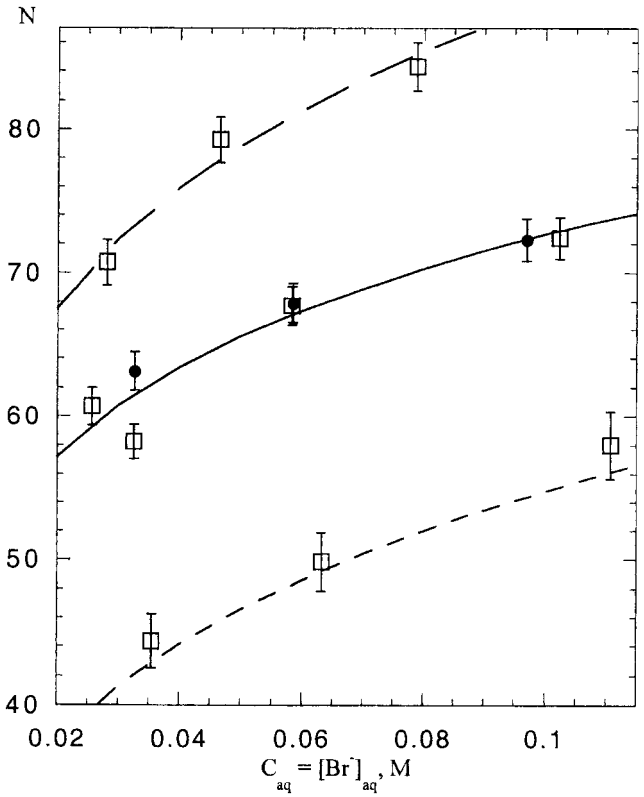

Figure 5. Aggregation numbers of DTAB versus the concentration of counterions in the aqueous phase at $T = 10.1$ °C upper points, $T = 25.0$ °C middle points, $T = 45$ °C lower points. Open squares zero NaBr and filled circles added NaBr. The lines are linear least-squares fits to eq 26 weighted by the inverse square of the uncertainties yielding the parameters N^0 and γ in Table 5.

TRFQ. Table 4 gives the values of the aggregation numbers for DTAB with and without added NaBr at 25 °C. Results are also presented for DTAB without added NaBr at 10.1 and 45 °C. Estimated relative uncertainties in N due to sample preparation and analysis are ±2% at 10.1 and 25 °C; and ±4% at 45 °C. In addition, there is a systematic error in the computation of *N* from eq 1 due to the uncertainties in the values of S_f which are dominated by the uncertainties in the values of cmc_0, column 5 of Table 5. These two uncertainties were added in quadrature to arrive at our final estimate of the relative uncertainties in *N*. Figure 5 shows the aggregation numbers versus $C_{aq} = [Br^-]_{aq}$ computed from eq 21 using the values of α corresponding to each temperature determined by EPR, Table 3. The lines are linear least-squares fits to eq 26 yielding values of γ and N^0 given in Table 5. Because both salt and surfactant were varied at 25 °C, TRFQ may also be used to measure α using eq 24. In this case, the schematic procedure of Figure 2 is applied to the aggregation numbers themselves. A plot of the squared deviations of the aggregation numbers from a trial function of the form of eq 26, similar to Figure 4, (not shown), has a minimum at $\alpha = 0.22$ with an estimated error of ±0.03. The error is larger in this case due to severely restricted statistics, but nevertheless shows that the EPR and TRFQ determinations of α based on eq 24 are consistent with one another.

TABLE 5: Values of N^0, γ, and cmc_0

	T, °C	N^0	γ	cmc_0, mM
DTAB	10.1	64.3 ± 2.6[a]	0.169 ± 0.03[a]	15.0 ± 1.0(2)[b]
DTAB	25.0	54.7 ± 1.6[a]	0.146 ± 0.02[a]	14.9 ± 0.5(4)[c]
DTAB	45.0	35.9 ± 1.1[a]	0.236 ± 0.02[a]	16.7 ± 1.2(4)[d]
DTAC	25	45.1[e]	0.112[e]	20.3 ± 0.9(4)[f]

[a] Fit to eq 26 weighted by the inverse squares of the uncertainties in *N*; uncertainties are standard error estimates from the fits. [b] Average: surface tension[80] and conductivity;[66] uncertainty assumed to be 1 mM because only two data points are available. [c] Average: surface tension and specific conductivity[80] and conductivity.[66] [d] Average: surface tension, specific conductivity, and turbidity plot[80] and conductivity.[66] [e] Fit of literature data[61] to eq 26. [f] Average: turbidity, surface tension, and specific conductivity measurements[80] and conductivity and light scattering.[81]

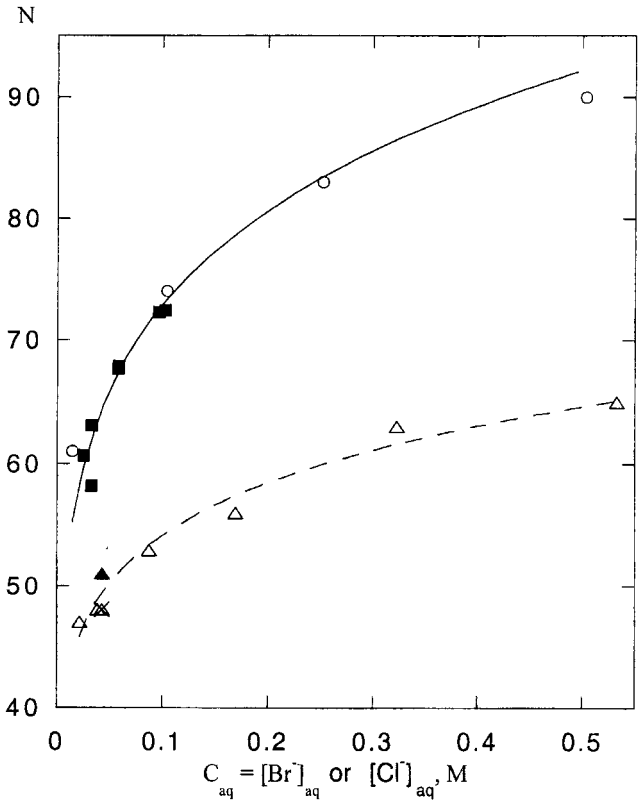

Figure 6. Aggregation numbers vs the concentration of counterions in the aqueous phase. Upper points and solid line, DTAB; TRFQ data, ■ (both salt-free and salt-added) light scattering data[59] ○. Lower points and dashed line, DTAC; TRFQ data △,[61] ▲,[16] ×.[62] The solid line is the same as the solid line in Figure 4; i.e., the best fit to the TRFQ data in this work. The dashed line is a fit to eq 26 yielding values of N^0 and γ given in Table 5.

Figure 6 compares the aggregation numbers obtained for DTAB in this work with those found by light scattering[59] as well as literature values of N for DTAC. Note that the abscissa in Figure 6 is C_{aq} equal to $[Cl^-]_{aq}$ for DTAC and $[Br^-]_{aq}$ for DTAB. The solid line is a plot of eq 26 using $\gamma = 0.146$ and

TABLE 6: Literature Values of N for DTAB Micelles

[DTAB, mM	[NaBr], mM	$[Br^-]_{aq}$, mM[a]	$F(S_t)$[b]	N	eq 26[c]	method	ref
100	0	32.6	1.03	49.8	61.9	SANS[d]	38
50.0	0	21.5	1.02	65.0	58.2	TRFQ[d]	82
30.0	0	17.6	1.01	50.7	56.6	TRFQ[d]	60
100	0	32.6	1.03	65.5	61.9		
602	0	189	1.23	116.9	80.0		
14.6	0	14.9	1.00	61	55.2	LS[d]	59
4.36	100	104	1.00	74	73.3		
2.54	250	252	1.00	83	83.4		
1.67	502	503	1.00	90	92.3		
50.0	0	21.5	1.02	57	58.2	SANS[f]	32
100	0	32.6	1.03	68	61.9		
200	0	58.4	1.07	69	67.4		
200	100	163	1.07	76	78.2		
400	0	118	1.14	75	74.7		
400	100	231	1.14	78	82.4		
600	0	189	1.22	75	80.0		
600	100	310	1.22	82	86.0		
50.0	0	21.5	1.02	47	58.2	SANS[d]	40
100	0	32.6	1.03	51	61.9		
200	0	58.4	1.07	55	67.4		

[a] Calculated from eq 21 using $\alpha = 0.257$ and $cmc_0 = 14.9$ mM. [b] Equation 22. [c] Employing $\gamma = 0.146$ and $N^0 = 54.7$, Table 5. [d] 25 °C. [e] Interpolated between 20 and 30 °C. [f] 40 °C.

TABLE 7: Literature Values of N for DTAC Micelles

[DTAC], mM	[NaCl], mM	$[Cl^-]_{aq}$, mM[a]	$F(S_t)$[b]	N	eq 26[c]	method	ref
31.0	0	23.4	1.01	47	45.9	TRFQ[d]	61
31.0	20.0	40.1	1.01	48	48.8		
31.0	72.0	89.1	1.01	53	53.3		
31.0	155	171	1.01	56	57.4		
31.0	310	326	1.01	63	61.7		
31.0	520	537	1.01	65	65.2		
100	0	45.6	1.03	51	49.5	TRFQ[e]	16
100	0	45.6	1.03	48	49.5	TRFQ[f]	62
50.0	0	29.0	1.01	57	47.0	TRFQ[f]	82
200	0	82.8	1.06	60	52.9	SANS[g]	32
200	100	186	1.06	60	57.9		
400	0	167	1.12	59	57.2		
400	100	278	1.12	61	60.6		
600	0	264	1.19	67	60.2		
600	100	382	1.19	67	62.8		
50.0	0	29.0	1.01	32	47.0	SANS[f]	40
100	0	45.6	1.03	37	49.5		
200	0	82.8	1.06	40	52.9		

[a] Calculated from eq 21 using $\alpha = 0.365$ and $cmc_0 = 20.3$ mM. [b] Equation 22. [c] Employing $\gamma = 0.112$ and $N^0 = 45.1$, Table 5. [d] 23 °C. [e] Interpolated between 20 and 30 °C. [f] 25 °C. [g] 40 °C.

$N^0 = 54.7$; i.e., the values found in the present work for DTAB at 25 °C. Other literature values of N for DTAB are gathered in Table 6. The sixth column is the predicted value of N from eq 26 using $\gamma = 0.146$ and $N^0 = 54.7$. Comparing these predictions with the literature data shows that the various techniques are generally in reasonable agreement with one another, except for one point from ref 60 that appears to be in error. Leaving out this point, all of rest of the data in Tables 5 and 6 show a 3.8 molecule root-mean-square departure from the prediction of eq 26.

Values of N for DTAC taken from the literature are presented in Table 7. Figure 6 also includes a plot of the TRFQ data.[16,61,62] The abscissa is $C_{aq} = [Cl^-]_{aq}$ computed from eq 21 using the value of $\alpha = 0.365$ determined by EPR. The dashed line is a fit of the data to eq 26 yielding the values of $\gamma = 0.112$ and $N^0 = 45.1$ which are tabulated in Table 5. The sixth column of Table 7 is the predicted value of N from eq 26 using $\gamma = 0.112$ and $N^0 = 45.1$. The data in Table 7 show a 4.5 molecule root-mean-square departure from the prediction of eq 26. In Tables 6 and 7, SANS data from one lab[32] are in good agreement with eq 26, whereas those from another lab[40] are consistently lower by 20−30%.

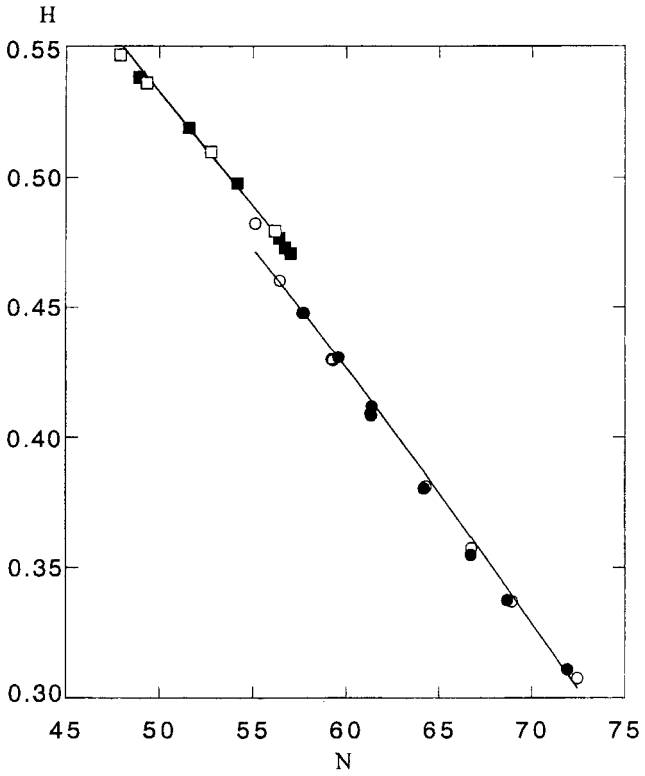

Figure 7. Volume fraction of the polar shell occupied by water versus the aggregation number of DTAB ○ and ●; and DTAC □ and ■. Open symbols, salt-free; filled symbols, salt-added. The solid line through the DTAB data is the best fit to eq 11; the solid line through the DTAC points is the same line scaled to take into account the difference in volume occupied by the bromide and chloride counterions. $T = 25$ °C.

Hydration of Polar Shell. From the values of A_+ in Figure 3, the polarity indices H for the two surfactants were computed from eq 4. These are plotted versus the aggregation numbers for the two surfactants in Figure 7. The data in Figure 7 are derived from various combinations of surfactant and salt concentrations so the hydration in cationic micelles depends only on their aggregation number, not on the micelle concentration. The simple geometric model that we have employed would predict a single curve in Figure 7 for the two surfactants if their counterions occupied a negligible volume as was the case for LiDS and SDS.[31] Here, however, the counterion volumes are neither negligible nor equal. They occupy different fractions of the polar shell for two reasons: the chloride ion is smaller and there are fewer of them in the polar shell. These two effects are combined in the quantity $V_{dry}{}^0$. A break in the curve was expected a priori just in the sense revealed by Figure 7; i.e., $V_{dry}{}^0$ for DTAC is smaller and displaces less water leading to a higher value of H. Quantitatively, to predict the difference in the two curves, one would have to know the relative thickness of the two polar shells; a difference far smaller than the uncertainty in the thickness. Therefore, to put the two surfactants on the same footing, we assume that the shell thickness and the fraction of methylenes residing in the polar shell scale as the diameter of $V_{dry}{}^0$; i.e., as $V_{dry}{}^{1/3}$. According to Table 2, this would give a reduction of $(124\ Å^3/135\ Å^3)^{1/3} = 0.972$ in the shell thickness and the number of methylenes in the polar shell.

The solid line in Figure 7 through the data points for DTAB is the theoretical prediction, eq 11 found by trial and error

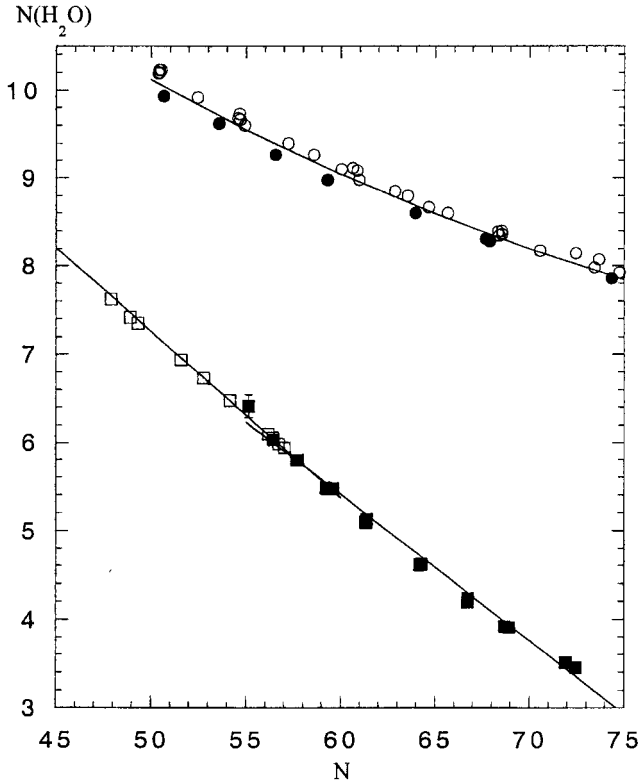

Figure 8. Number of water molecules per surfactant molecule in the polar shell of DTAB, ■; DTAC, □, SDS,[5] ○, and LiDS,[31] ●. For clarity, salt-free and salt-added samples are not distinguished; there is about an even mixture of the two types of samples. $T = 25$ °C.

utilizing eqs 8−10 beginning with the reasonable assumption that $N_{wet} = 0$ at $N = 0$. Thus, $N_{wet}{}^0 = \partial N_{wet}/\partial N\, N^0$ in eq 9. The consequences of choosing other values of $N_{wet}{}^0$ are treated in the Appendix. The parameters $\partial N_{wet}/\partial N$ and the shell thickness were varied to achieve the best accord between theory and experiment. The best fit yielded $\partial N_{wet}/\partial N = 0.051$ and a shell thickness $R_m - R_c = 5.35$ Å. The behavior of eq 11 is quite different under the variation of the thickness and $\partial N_{wet}/\partial N$ so it is easy to find the best fit. Essentially, the thickness controls the vertical position of the solid line in Figure 7, whereas $\partial N_{wet}/\partial N$ makes minor changes in the slope. Next, for DTAC, we have scaled $\partial N_{wet}/\partial N$ to (0.972)(0.051) = 0.050 and the shell thickness to (0.972)(5.35) = 5.20 Å. The line through the experimental points for DTAC is eq 11 without any further adjustments in the parameters; i.e., it is the continuation of the curve for DTAB under the scaling for the difference in $V_{dry}{}^0$ for the two counterions.

Figure 8 shows the values of N_{H_2O} for the two surfactants as a function of their aggregation numbers. In this figure, both salt-containing and salt-free data are combined. The continuity in the values of N_{H_2O} in passing from DTAC to DTAB shows that the hydration of the DTA^+ micelle is the same for Cl^- and Br^- at the same value of N. This fact tends to support the conclusion of ref 31 that specific ion interactions do not affect the value of A_+ as given by eq 4. If there were specific interactions, one would expect differences in the values of A_+ for the same value of H. The theoretical lines computed from eq 13, appear to be straight lines even though eq 11 is nonlinear since the range of N is limited. It is important to bear in mind that points of overlap of DTAB and DTAC aggregation numbers are taken with very different concentrations of counterions in the aqueous phase. For example, the points near $N = 57$ in Figure 8 correspond to $[Cl^-]_{aq} = 144$ mM, whereas $[Br^-]_{aq} = 21.7$ mM; i.e., a difference of a factor of nearly 700% in the concentration of counterions in the aqueous phase is required to produce the same micelle size with the two counterions. This underlines the fact that hydration is indirectly connected with added salt through the dependence of N on C_{aq}. Corresponding hydration data for SDS and LiDS taken from the literature[31] are also shown in Figure 8 for comparison. Compared with SDS and LiDS,[5] the cationic micelles are dryer and decrease in hydration faster with micelle size.

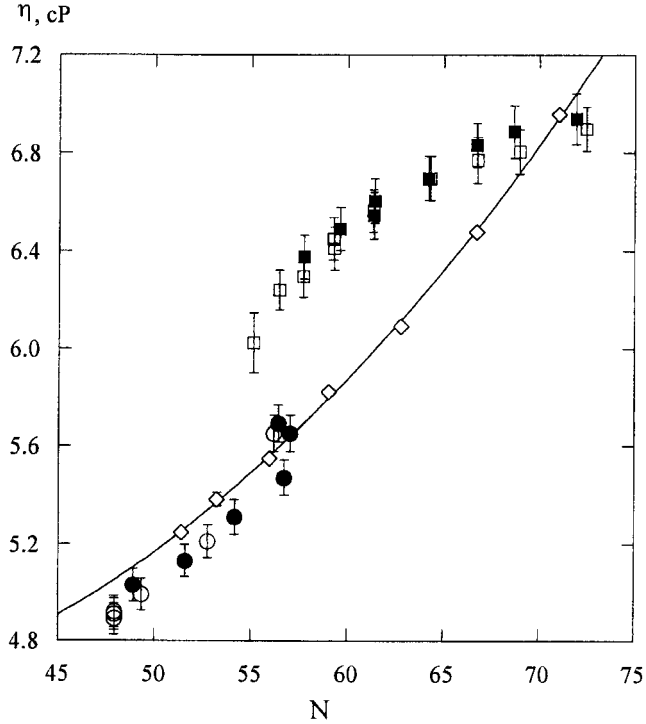

Figure 9. Microviscosity of the polar shell of DTAB, □ and ■; DTAC, ○ and ●; and SDS, ◇. Open symbols salt-free, closed symbols added salt. The solid line is to guide the eye through the SDS data. $T = 25$ °C.

Microviscosity of Polar Shell. Values of $\tau_{measured}$ were obtained as a function of C_{aq} for DTAC and DTAB at 25 °C. A few measurements were also taken with DTAB at 10.1 °C and 45 °C. Microviscosities were computed from eq 14 using eqs 15 and 16. The ratio τ_B/τ_C, obtained from two independent measurements of the rotational correlation time τ_B and τ_C,[27] differed from unity by less than ±1% for DTAB at 10.1 °C, ±2% for DTAB at 25 and 45 °C, and ±3% for DTAC at 25 °C. Thus the reorientation of the nitroxide group in these two micelles is very nearly isotropic. Figure 9 shows the variation of the microviscosity as a function of N for the two surfactants at 25 °C. The measured microviscosities are the same in salt-free and salt-added samples. A brief experiment with SDS was performed in the absence of salt at low values of [SDS], ranging from 200 mM down to 15.8 mM (~2 × cmc_0) in order to compare the viscosities of the three surfactants over the same range of N. The values of the viscosity were derived in the same way using the same spin probe. The results are shown with diamonds in Figure 9; the line is a quadratic fit to guide the eye. The abscissa for Figure 9 is computed from eq 26 using the appropriate values of α, γ, and N^0 for the three surfactants in eq 21; Table 3 for DTAC and DTAB and $\alpha = 0.27$, $\gamma = 0.25$, and $N^0 = 49.5$ for SDS.[19] The average values of the microviscosity for DTAB at 10.1 and 45 °C were 12.2 ± 0.8 and 3.2 ± 0.1 cP, respectively.

Quenching Rate Constants. Table 8 gives the values of the quenching rate constants of Py by $C_{16}PC$ from this work and

TABLE 8: Quenching Rates, Viscosities, Core Radii, and Shell Volumes for DTAB and DTAC Micelles

S_t, M	C_{ad}, M	T, °C	k_q, 10^7 s^{-1}	R_c, Å	η, cP	V_{shell}, 10^4 Å^3
DTAB	NaBr					
100	0	10.1	1.47 ± 0.07		12.2 ± 0.1	
200	0	10.1	1.30 ± 0.07		12.2 ± 0.1	
350	0	10.1	1.19 ± 0.06		12.2 ± 0.1	
100	0	25.0	3.00 ± 0.15	15.6[a]	6.35 ± 0.32	2.25[a]
200	0	25.0	2.52 ± 0.13	16.1[a]	6.84 ± 0.35	2.38[a]
350	0	25.0	2.33 ± 0.12	16.3[a]	6.90 ± 0.35	2.44[a]
70.0	0	25.0	3.0 ± 0.15	15.7[a]	6.53 ± 0.33	2.28[a]
70.0	8.04	25.0	2.77 ± 0.14	15.8[a]	6.66 ± 0.33	2.32[a]
70.0	35.5	25.0	2.55 ± 0.13	16.1[a]	6.84 ± 0.34	2.38[a]
70.0	74.4	25.0	2.42 ± 0.12	16.3[a]	6.90 ± 0.35	2.44[a]
100	0	45.0	6.3 ± 0.6		3.2 ± 0.1	
200	0	45.0	5.3 ± 0.5		3.2 ± 0.1	
350	0	45.0	5.6 ± 0.6		3.2 ± 0.1	
DTAC	NaCl					
31.0	0	23	5.00	14.9[b]	4.83 ± 0.24	1.93[b]
31.0	20.0	23	4.73	14.9[b]	4.90 ± 0.25	1.95[b]
31.0	72.0	23	4.17	15.3[b]	5.26 ± 0.26	2.04[b]
31.0	155	23	3.60	15.5[b]	5.47 ± 0.27	2.09[b]
31.0	310	23	3.17	16.0[b]	5.97 ± 0.30	2.19[b]
31.0	520	23	3.17	16.1[b]	6.11 ± 0.31	2.22[b]

[a] Computed using $N_{wet}^0 = 2.8$, $\partial N_{wet}/\partial N = 0.051$, $R_m - R_c = 5.35$ Å. [b] $N_{wet}^0 = 2.2$, $\partial N_{wet}/\partial N = 0.050$, $R_m - R_c = 5.20$ Å.

of 1-MePy by C_{14}PC from the literature.[61] Figure 10 shows a plot of these rates versus $8RC_QT/3000\eta$, where the viscosity is taken from Figure 9. The straight line is a least-squares fit to eq 20 for the combined data of DTAB (25 °C)and DTAC (23 °C) yielding a quenching probability of $P = 0.4$ with a coefficient of correlation $r = 0.978$. Considering that the data for the two surfactants were obtained by two different labs[61] using two different quenchers (C_{16}PC vs C_{14}PC) on two different fluorophores (Py vs 1-MePy); the adherence of the data to the Stokes−Einstein−Smolukhovsky equation at 23 and 25 °C is excellent. The data for DTAB at 10.1 °C fall nicely on the same line as the 25 °C data; however, the 45 °C data show about a 10% smaller quenching rate than the solid line. The uncertainties in the quenching rates in Figure 10 are estimated to be ±5% at 10.1 and 25 °C and ±10% at 45 °C. The uncertainties in the abscissa were estimated as follows: a ±1°K error in the temperature leads to a ±4% error in η. An error of ±0.5 Å in holding the thickness constant contributes an error in V_{shell} of about 7% and a similar error results in assuming that the thickness is constant as a function of T. A 10% error in V_{dry}^0 contributes another 3% error in V_{shell} because an adjustment in $R_{micelle}$ is needed to keep H in accord with experiment. This results in uncertainties of ±9% for the 25 and 23 °C data and ±13% for 10.1 and 45 °C data. These error bars indicate the relative uncertainties of the values plotted. The absolute error could be as much as ±25°.

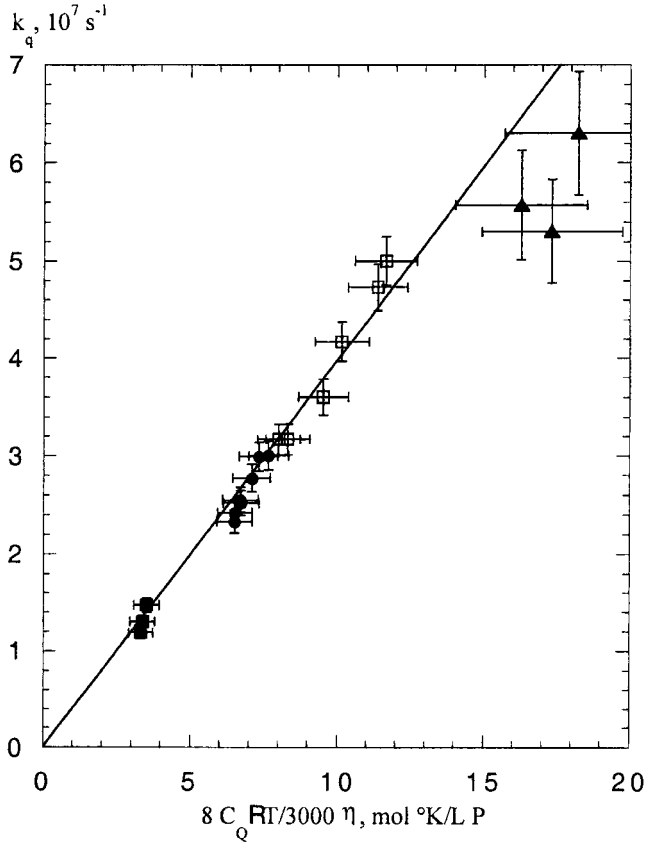

Figure 10. The fluorescence quenching rate of Py by C_{16}PC in DTAB at 10.1 °C, ■; 25.0 °C, ●; 45 °C, ▲, and of 1-MePy by C_{14}PC in DTAC at 23 °C, □ versus $8C_Q$ $RT/3000\eta$. The straight line is a linear least-squares fit of the combined DTAB and DTAC data at 25 and 23 °C to the Stokes−Einstein equation, eq 20, yielding a probability of quenching per collision $P = 0.4$. The molar concentration C_Q is due to one quencher in the volume defined by the polar shell and the viscosity is determined by the rotational motion of a nitroxide spin probe. A plot of the same data with C_Q calculated using the entire micelle volume rather than that of the polar shell yields a similar curve with $P = 0.7$.

Discussion

Aggregation Number-Based Definition of α. Equation 25, as implemented for constant α, eq 24, appears to work well for both DTAB and DTAC. For DTAB at 25 °C, the values given by EPR and by TRFQ agree within experimental error with one another and with values taken from the literature. See Table 3. Some of the values in Table 3 were derived from the well-known[63] dependence of the cmc on C_{ad} as follows

$$\log(\text{cmc}) = -K_3 - K_4 \log(\text{cmc} + C_{ad}) \qquad (27)$$

where K_3 and K_4 are constants. An approximate value of α may be obtained from eq 27 because mass action theory predicts that $K_4 \approx 1 - \alpha$ in the limit of large aggregation numbers.[20,21] The literature values are collected together and averaged according to the method except that the results of Gaillon et al.[64,65] are listed separately because they compare the values of α derived from eq 27 and potentiometric measurements using the same materials and sample preparations. For DTAB, these authors[64,65] report α = 0.38 from eq 27 and 0.23 from potentiometric measurements. Uncertainties were not reported;[64,65] however there appears to be a significant difference. This difference is also found from other values of α in Table 3 where α = 0.35 ± 0.11 from eq 27 and α = 0.242 ± 0.028 from all other methods excluding the present results. Our value from EPR and TRFQ, 0.244 ± 0.019 compares well with this latter value. For DTAC, the difference in values of α derived from eq 27 and other methods is insignificant. Our value derived from EPR α = 0.365 ± 0.008 compares with the unweighted mean of all other values in Table 3 α = 0.36 ± 0.05. The results of Table 3 support the contention[64,65] that, in some cases, eq 27 does not provide a reliable estimate of the value of α. We found only one set of data[66] with which to compare our results at 10 and 45 °C. These data, derived from specific ion electrode measurements,[66] are presented in Table 3. They agree well with the present results at 25° and reasonably well at 10.1 and 45 °C. The slope of the α vs T curve, $\partial\alpha/\partial T$, is similar for the values from the literature,[66] $\partial\alpha/\partial T = 0.0026$ °K^{-1}, and the present values from EPR, $\partial\alpha/\partial T = 0.0024$ °K^{-1} over the range

10 to 45 °C. These are also similar to the value $\partial\alpha/\partial T = 0.0033$ $°K^{-1}$ for tetradecyltrimethylammonium bromide measured by one of us.[67]

There are several reasons why the aggregation number-based definition of α is of interest. First, the definition is independent of the experiment technique, not involving a decision on where and for how long the counterions reside. Second, as implemented by EPR, it is an extremely easy experiment. Due to the simplicity of the method, it becomes feasible to investigate large numbers of systems varying a number of experimental parameters such as the temperature, chain length, counterion, and added non electrolytes. The EPR technique can be performed using very small amounts of material. A typical sample in this work is of volume 50 μL because 50 μL disposable pipets are used to house the sample; however, this could be easily reduced to 20 μL using the same pipets. The use of flat cells would reduce the requirements further. Thus, for expensive or rare surfactants, quite small amounts of material could be used, the limiting factor being the precise determination of the concentrations. In the EPR approach, one works well above the cmc, so impurities are less of a problem than in techniques working near the cmc. The disadvantage of EPR, and in any method employing eq 24, is that one cannot evaluate α at surfactant concentrations near the cmc.

Micelle Growth with C_{aq}. Equation 26, with parameters given in Table 5, describes the growth of DTAC and DTAB micelles in the slow growth regime, below any possible sphere-rod transitions. There are a number of advantages to having an accurate empirical description of micelle growth. The aggregation numbers from different combinations of salt and surfactant may be predicted in the planning of experiments. It offers a method to reevaluate existing data as a function of N, even though the original interpretation was based on different aggregation numbers, or if a constant value of the aggregation number was assumed. Equation 26 may prove to be valuable in experiments in which either salt or surfactant concentrations are varied in order to derive the slope of some experimental variable. For example, using viscosity measurements to investigate micelle hydration,[42,68−70] it is common to vary the surfactant concentration in the presence of salt. In conductivity measurements to study α,[71] the surfactant concentration is varied through the cmc_0 in the absence of salt. Often the assumption has been made that N does not vary in analyzing the slopes of quantities derived in such experiments but, there is no longer any need for the assumption. Figure 6 illustrates a practical advantage: the values of the aggregation numbers derived from different techniques working over very different concentration ranges can be easily compared. To illustrate, for DTAB, consider the three points in the vicinity of $N = 72-74$ of Figure 6. These three points were derived from samples prepared with three surfactant salt combinations as follows: [DTAB]/[NaBr] = 350/0, 70/97, and 4.36/100 in units mM/mM. Thus, for these three samples having similar aggregation numbers, there is an 80-fold difference in surfactant concentrations resulting in micelle concentrations ranging from near zero to about 4.8 mM. At this latter concentration, the micelles are getting to be quite crowded. Using a simple cubic lattice, at 4.8 mM, the center-to-center micelle distance is about 68 Å, compared with the micelle diameter $2R_m = 43$ Å. Thus, ionic inter micelle interactions, even when the micelles are quite crowded, have a negligible effect on micelle aggregation numbers. This result is not surprising because the Debye−Hückel screening length, which describes the distance over which the electrostatic interaction is attenuated,[53] is less than 10 Å at 25 °C with $C_{aq} = 100$ mM.

In eq 26, the meaning of N^0 is clear. There is a need for a theoretical understanding of γ, if any. With a lack of such understanding, it is important to avoid over interpreting γ. Further, accurate values of γ are not easy to obtain because they are very sensitive to the values of N at low vales of C_{aq}; i.e., at low values of S_t in the absence of salt. This is the region in which the purity of the material becomes very important because of the influence of impurities on the cmc_0. With the TRFQ technique low values of S_t pose another problem because the factor $S_t - S_f$ in eq 1 becomes subject to large error. To illustrate, we take the determination of N^0 and γ for DTAC from the data in Table 7 as an example. A typical uncertainty of 10% in S_f leads to an uncertainty in the value of N^0 of 8% and in γ of 22%. Light scattering avoids this problem near the cmc_0, but the problem of purity persists. The problem does not arise in SANS, but the reproducibility of N is poorer. See Tables 6 and 7.

Microviscosity of the Polar Shell. The microviscosity of the polar shell increases modestly for both DTAC and DTAB as the micelles grow, similar to the increase observed for SDS, Figure 9. This viscosity increase is minor compared with viscosity increases observed for surfactant mixtures of SDS and a sugar-based nonionic surfactant where a variation of about a factor of 5 was observed as a function of the composition.[3] These results predict that molecules housed in the polar shell would rotate about a factor of 6−7 slower than in pure water. NMR relaxation times have been interpreted[34] to mean that water at the surface of micelles reorient typically about 2−3 times slower than in the bulk. Because the analysis of the relaxation data requires a number of assumptions[34] and water exchanges between the shell and the bulk, the agreement is satisfactory. For DTAB, we have limited data as a function of temperature; however, they are interesting and worthy of brief discussion. The variation of η with N is much smaller than its variation with T, so we averaged the values of η at each the three temperatures to obtain $\eta = 12.21 \pm 0.08$, 6.58 ± 0.25, 3.20 ± 0.13 cP for $T = 10.1$, 25.0, and 45.0 °C, respectively. A plot of the logarithm of these values versus $1/T$ produces an excellent linear plot (not shown) with coefficient of correlation $r = 0.999$ adhering to the classical expression of activated viscosity

$$\eta = \eta_0 e^{B/RT} \tag{28}$$

with $B = 29.1$ kJ/K mole. In contemplating the nature of the liquid that the polar shell of DTAB presents to a guest molecule, we compared this activation energy with those found in ethanol−water mixtures taking data from the literature.[72] Ethanol−water mixtures adhere well to eq 28 as a function of temperature, producing values of B that are approximately constant as a function of wt % EtOH except for mixtures near pure water or ethanol. For example, from 20 to 60 wt % ethanol, B has a mean value of $B = 23.8 \pm 1.2$ kJ/K mole where the uncertainty is the standard deviation in 5 mixtures. The average coefficient of correlation in the linear least-squares fit to eq 28 over these 5 values is $r = 0.995 \pm 0.003$. Therefore, with respect to the activation energy of viscosity, the polar shell of DTAB is a rather normal liquid mixture, not very different than ethanol−water mixtures. Note that the microviscosity activation energy for DTAB, measured using the rotation of the relatively small doxyl group in this work is smaller than that reported by a much larger fluorescent probe.[73]

Hydrodynamic Description of Bimolecular Collisions in Micelles. The quenching rates of Py by $C_{16}PC$ in DTAB at 25 °C and of 1-MePy by $C_{14}PC$ in DTAC at 23 °C are in excellent agreement with the prediction of eq 20 which is given as the solid line in Figure 10. It may be partially fortuitous that the

quenching rates for the two surfactants using different quencher-fluorophore pairs is described by the same Stokes−Einstein equation because temperature control is important and the DTAC data were obtained at room temperature.[61] Note, however, that the size of the diffusing molecules does not enter into eq 20, so a strong dependence is not predicted by theory. Given the uncertainties, even the data at 10.1 and 45 °C are well predicted by eq 20.

Note that the value of $P = 0.4$ results from the fact that we have assumed that the polar shell thickness found by adjusting the polarity to that of the model is the same that bounds the diffusional motion of the fluorophores and the quenchers. We have also assumed that the microviscosity estimated from the rotation of the spin probe is the appropriate viscosity to use in eq 20. This, in turn, assumes that the spin probe reports an average viscosity over the same volume occupied by fluorophores and the quenchers. If, in fact, the effective volumes for the motion of the various probes are somewhat different and that the effective volume is something different than the polar shell, the numerical value of P would be altered. For example, introducing an uncertainty in the shell thickness of ±0.8 Å results in uncertainty in P of about 20%. Quenchers such as C_{16}PC and C_{14}PC that are charged and are themselves surfactants could be expected to undergo excursions from the polar shell into the aqueous phase more frequently than 16DSE and Py which are hydrophobic. This would have the effect of increasing the volume through which the molecules diffuse in the hydrodynamic formulation; i.e., the volume in eq 19 would be larger than V_{shell}. If we suppose that the two molecules diffuse through the entire volume of the micelle, a graph very similar to Figure 10 results and the fit to eq 20 is of a similar quality ($r = 0.983$); however, the probability of quenching increases to $P = 0.70$. One arrives at the results by replacing V_{shell} with $V_{micelle}$ in eq 19. The discrepancy of the 45 °C data becomes slightly worse, now being about 14% below the Stokes−Einstein prediction from the 25 °C data. Thus from the quality of fit to eq 20 alone, one cannot distinguish between a model of polar shell diffusion and diffusion throughout the entire micelle. Both descriptions work equally well; the range of values of N is not sufficiently large to distinguish the difference in the variations of V_{shell} and $V_{micelle}$, respectively.

It is important to note that uncertainties in the volume through which the molecules diffuse do not affect the linearity of the curve in Figure 10, only the slope is changed. In other the words, the Stokes−Einstein equation is valid in any case. DTA^+ micelles offer a reaction medium in which one can predict the relative collision rates of two hydrophobic molecules at different salt and surfactant concentrations and at different temperatures. Obviously, molecules that partition appreciably into the aqueous pseudophase would have to be treated appropriately.

Hydration of Micelle Surfaces. The fundamental quantity reported by the spin probe is the volume fraction occupied by water, Figure 7. This is the important parameter which characterizes the DTA^+ micelle as a reaction medium within the polar shell. Whether a guest molecule encounters this volume fraction of water depends on whether it occupies the same average position in the micelle as the spin probe. The interpretation of the decrease in H as the micelles grow is that the available volume per surfactant in the polar shell decreases, expelling water. Figure 7 shows that DTAC and DTAB are similarly hydrated as a function of N, as would be required, a priori, by the simple geometrical model employed.

In comparing the measured value of H to theoretically predicted values given by the solid line in Figure 7, the core−shell model is employed. The detailed description of the hydration of micelles rests on the classical model originally proposed by Hartley.[33] The claim was already made 20 years ago[34] that "the overwhelming majority of experimental and theoretical studies have confirmed the classical picture", thus we consider the basic model to be sound and have proceeded to seek more details. We discussed[5] in some detail the assumptions and uncertainties involved in the use of the model as well as proposed[5] a number of severe experiment tests of the model. To reiterate briefly, our interpretation of the core−shell model assumes that the spin-probe samples all regions of the polar shell. The growing conviction that this is a reasonable assumption stems from the fact that the curve through data for SDS and LiDS in Figure 8 has no adjustable parameters once V_{dry} is fixed. Further, the model has predicted the behavior of H and N_{H_2O} as sugar-based headgroups are inserted into SDS micelles.[3,29] Nevertheless, the decrease in the values of H in Figure 7 and N_{H2O} in Figure 8 could conceivably arise due to subtle changes in the average position of the probe as the micelle grow. In this interpretation, one would have to assume that both the position of the probe and the departure of the hydration from the simple model of Figure 1 would have to vary in such a compensatory manner as to leave the curve in Figure 8 for SDS and LiDS unchanged. Because this is very unlikely, we have persisted in the use of the original model. In applying the same model to cationic micelles, we tacitly assume that the average probe position remains the same during micelle growth in this case as well. Here, the arguments that this is true are not yet as well established. First, the curves through the points in Figures 7 and 8 are not computed without any adjustable parameters in addition to V_{dry}. We must postulate that hydrocarbon from the surfactant tail occupies the polar shell. This is a reasonable postulate, being in accord with numerous other experimental papers[32,36−40] as well as being predicted by a theoretical cell model[74] and by molecular dynamics simulations.[75] Nevertheless, we urge caution in interpreting Figure 8 until more work has been done. The same tests of the core−shell model that were outlined in ref 5 for SDS may be carried out for DTAB and DTAC in order to substantiate the model.

Note that the core radius, tabulated in Table 8 is always less than the fully extended length of a twelve-carbon chain 16.7 Å,[43] so the problem of maintaining a spherical micelle[43] does not arise in DTAC or DTAB over the range of N studied here.

The data in Figure 8 support the long standing,[69] generally accepted[42] picture that monovalent counterions retain their hydration when occupying the polar shell. If we take the primary hydration numbers suggested by Hayter and Penfold; 4 for Cl^- and Br^- (resulting in about $(1 - \alpha)4 \approx 3$ within the polar shell) and 1 for the headgroup, then we arrive at a constant value of primary waters of hydration of about 4. Thus "free" water, that is the water in excess of $N_{H_2O} = 4$, is estimated from Figure 8 to decrease from about 4 to near zero in going from $N = 48$ to 72. The absolute values of N_{H_2O} are dependent upon the model employed for the micelle as well as the numerical values of the parameters as discussed above. The entire curve of Figure 8 could easily move up or down by 25% employing reasonable estimates of the uncertainties involved; however, the relative values of N_{H_2O} are quite precisely determined.

Micelle hydration has been studied by transport properties[42] taking the micelle hydration number as the number of water molecules moving as a kinetic unit with the micelle.[42] For example, using viscosity data, Mukerjee[69] estimated $N_{H_2O} = 5$ for DTAC. The method involved extrapolation to zero micellized surfactant and using salt to reduce the electroviscous effect. Not

enough information was given to allow us to place this datum in Figure 8; however, it probably falls toward the top of the range of $N = 47-57$ where the agreement with the present data must be consider satisfactory. Contrasting this result is the work of Güveli et al.[76] who used the same technique to estimate much larger values of $N_{H_2O} = 31$ for DTAB. The authors[76] mention the electroviscous effect but it is not clear if they accounted for the effect. Hydration numbers are often reported together with SANS experiments either by assigning values of primary waters of hydration to the constituents[32] or by using the same model used here.[38] Unfortunately, the resulting estimates from this latter approach range from $N_{H_2O} = 0$ for tetradecyltrimethylammonium bromide[77] to $N_{H_2O} = 19$ for DTAB.[38] Worrisome when considering the SANS approach, is the fact that Berr[38] has shown that same scattering profile can be satisfactory fit with or without water in the polar shell.

Chemical trapping results on DTAC or DTAB will be eagerly awaited. The hydration numbers reported by chemical trapping, employing a charged probe, are not expected to be the same as those reported by EPR, employing an uncharged hydrophobic probe. The charged probes surely have a higher probability of occupying the aqueous phase. It is the variation of hydration numbers with N that will be informative; both approaches interpreted using the core−shell model, albeit occupying different average positions within the polar shell, must to lead to predictable dehydration as the micelles grow.

Conclusions

Very different concentrations of counterions in the aqueous phase are required to produce DTAB and DTAC micelles of the same aggregation number; however, the two micelles present the same hydration and nearly the same microviscosity to a guest molecule as a function of N. According to the simple core−shell model, the hydration, expressed as the number of molecules of water per surfactant molecule, decreases from about 7.5 to 3.5 over the range $N = 48$ to 73. The microviscosity increases from about 5 to 7 cP as the micelles grow over this same range, similar to SDS. The major difference manifest by the different counterions is their degree of dissociation from the micelle: about 26% for Br^- and about 37% for Cl^-. A new method to measure the degree of counterion dissociation implemented by EPR and TRFQ yields these values which are in agreement with literature values. Values of N for DTA^+ micelles are a function of the concentration of counterions in the aqueous phase only for both Cl^- and Br^- and are well predicted by the power law eq 26. For DTAB, N^0 decreases and α increases with temperature. Guest molecules in DTA^+ micelles collide with a rate that is described by the same Stokes−Einstein−Smolukhovsky equation for both Cl^- and Br^- with a quenching probability of 0.4 if the molecules are assumed to diffuse through the polar shell and 0.7 if they diffuse through the entire micelle. The activation energy associated with the viscosity in these micelles is similar to that observed in ethanol−water mixtures.

Appendix

Uncertainties in the Values of α using eq 24. Minima in graphical presentations such as Figure 3 may be determined to about ±2% in a given experiment; however, this minimum is only reproducible to about ±3% from one experiment to the next using different spin probes.[24,50] The overall accuracy in α using any technique based on eq 24 is limited by the uncertainty in the value of V in eq 22. For typical surfactants with molecular weights of 200−400, $F(S_t)$ amounts to a 5% correction when S_t reaches 125−250 mM. In this work, where we extend [DTAB] to values near 350 mM, the correction is as high as 12%. Ignoring the factor $F(S_t)$ completely in eq 24 for the data in Figure 3 leads to a 6.8% increase in the value of the minimum in Figure 4. Therefore, a 15% uncertainty in the value of V would add an additional uncertainty in the value of α of 1%. Adding, in quadrature, this uncertainty to those due to sample preparation and location of the minimum gives an overall estimated uncertainty of ±4% in the values of α determined by EPR.

TABLE 9: Possible Sets of Parameters Yielding the Solid Lines in Figure 7

$\partial N_{wet}/\partial N$[a]	$R_m - R_c$,[a] Å	$N_{wet}{}^{0}$[b]	wet terminal methyl groups[c]	wet methylene groups[c]	range of N_{H_2O}[d]
0.045	3.67	0.46	0.23	0.0	5.35−2.40
0.050	4.56	1.7	0.87	0.0	6.70−3.00
0.051	5.35	2.8	1.0	0.79	7.70−3.41
0.053	6.20	3.9	1.0	1.9	8.90−3.80
0.054	7.02	5.0	1.0	3.0	10.0−4.20
0.053	7.85	5.9	1.0	3.9	11.0−4.50
0.049	8.85	7.1	1.0	5.1	12.0−5.00

[a] DTAB. For DTAC, scale by 0.972. [b] DTAB. Model in which only methylene groups are wet. For DTAC, values are an average of 0.55 lower. [c] DTAB. Model in which the terminal methyl becomes wet first, followed by methylene groups. [d] Range of N_{H_2O} from $N = 47$ to 72.5 for both DTAB and DTAC.

Methylene versus Methyl Groups in the Polar Shell. To be definite, we have written eqs 5 and 10 in terms of the number of methylene groups occupying the polar shell; i.e., for situations depicted in Figure 1a and c. For a model in which the terminal methyl group occupies the polar shell, perhaps followed by methylene groups, depicted in Figure 1d, eqs 5 and 10 would be different in detail; however, there is not need to rewrite the theory. Once a value of N_{wet} is found, in the formalism of eqs 5 and 10, the number of terminal methyl groups is easily found by computing $V_{CH_2}N_{wet}/V_{CH_3}$, which according to Table 2 is very nearly equal to $N_{wet}/2$. Once the average number of terminal methyl groups exceeds unity, then the remainder of N_{wet} is allocated to methylene groups. In essence, if N_{wet} is less than 2, the number of methyl groups residing in the polar shell is $N_{wet}/2$ and above this, when the number of methyl groups becomes unity, the number of methylene groups becomes $N_{wet} - 2$. In Table 9, the third column supposes only configurations such as Figure 1a and c, whereas columns 4 and 5 refer to configurations such as Figure 1d.

Hydrocarbon Occupying the Polar Shell. The lines in Figures 7 and 8 were computed with the assumption that $N_{wet} = 0$ at $N = 0$, so $N_{wet}{}^0 = \partial N_{wet}/\partial N\ N^0$. Thus, $N_{wet}{}^0 = (0.051)(54.7) = 2.8$ for DTAB and $N_{wet}{}^0 = (0.050)(45.1) = 2.2$ for DTAC. If we now assume some other value of $N_{wet}{}^0$in eq 9 and refit the data, we arrive at the same solid lines through the data points in Figure 7 by adjusting the values of the shell thickness and $\partial N_{wet}/\partial N$. Figure 8 is identical using the new set of parameters, except the scale of the ordinate is different. Table 9 gives sets of possible values of $N_{wet}{}^0$, $\partial N_{wet}/\partial N$, and $R_m - R_c$ that fit the experimental data. Fixing any one of the parameters $\partial N_{wet}/\partial N$, $N_{wet}{}^0$, or $R_m - R_c$ either from independent experiments or by plausibility arguments fixes the other two.

From EPR alone, any of the combinations in Table 9 fit the data equally well; however, most of them are not reasonable. The possible values of $N_{wet}{}^0$ are bounded at one extreme by the physical requirement that N_{wet} not be negative and at the other extreme that N_{wet} be less than some reasonable value and certainly less than $N_c = 12$. If we argue that it is implausible to allow N_{wet} to be much bigger than say than $N_{wet} = 4$ of ref 40, then, from Table 8, $N_{wet}{}^0$ is restricted to the range 0.46 to 3.9

for DTAB. The two lines for DTAB and DTAC Figure 8 are essentially the same, so we discuss DTAB for the rest of the presentation; the footnote to Table 9 details the values for DTAC. The literature often reports that "about two methylene groups are fully exposed",[34,44] which in our case would point to a range of $N_{wet}^0 = 1.7$ to 2.8. If we further wish to respect the prevailing opinion[42] that the counterions retain their waters of hydration; i.e., $N_{H_2O} > 4$,[32] then this narrows the choices down to the range $N_{wet}^0 = 2.8$ to 3.9. Thus, $N_{wet}^0 = 2.8$ is a reasonable compromise. Figure 8 shows the results for $N_{wet}^0 = 2.8$; if we were to have used $N_{wet}^0 = 1.7$, then the values of N_{H_2O} would have shifted up by about 1.2 molecules at $N = 48$ and by about 0.4 molecules at $N = 73$. The *relative* values of N_{H_2O} are rather precise, about the size of the symbols in Figure 8.

For all of the possibilities in Table 9, the increase in the hydrocarbon that occupies the polar shell as the micelles grow from about $N = 47$ to 72.5 is approximately $\partial N_{wet}/\partial N \Delta N = (72.5-47)0.05 = 1.3$ methylene groups.

Acknowledgment. We gratefully acknowledge support from NIH/MBRS S06 GM48680-03, the Université Louis Pasteur, and the CNRS. Special thanks are due Philippe Turek and Maxime Bernard whose constant, cheerful support with the EPR measurements was invaluable.

References and Notes

(1) Soten, I.; Ozin, G. A. *Curr. Opin. Colloid Interface Sci.* **1999**, *4*, 325.
(2) Grieser, F.; Drummond, C. J. *J. Phys. Chem.* **1988**, *92*, 5580.
(3) Bales, B. L.; Ranaganathan, R.; Griffiths, P. C. *J. Phys. Chem. B* **2001**, *105*, 7465.
(4) Soldi, V.; Keiper, J.; Romsted, L. S.; Cuccovia, I. M.; Chaimovich, H. *Langmuir* **2000**, *16*, 59.
(5) Bales, B. L.; Messina, L.; Vidal, A.; Peric, M.; Nascimento, O. R. *J. Phys. Chem. B* **1998**, *102*, 10 347.
(6) Cuccovia, I. M.; da Silva, I. N.; Chaimovich, H.; Romsted, L. S. *Langmuir* **1997**, *13*, 647.
(7) Cuccovia, I. M.; Agostinho-Neto, A.; Wendel, C. M. A.; Chaimovich, H.; Romsted, L. S. *Langmuir* **1997**, *13*, 5032.
(8) Menger, F. M.; Keiper, J. S.; Mbadugha, B. N. A.; Caran, K. L.; Romsted, L. S. *Langmuir* **2000**, *16*, 9095.
(9) Romsted, L. S.; Yao, J. *Langmuir* **1996**, *12*, 2425.
(10) Binana-Limbélé, W. Doctorate Thesis, University Louis Pasteur, Strasbourg, 1991.
(11) R. Zana in *Surfactant Solutions: New Methods of Investigation*; Zana, R., Ed.; Marcel Dekker: New York, 1987; Vol. 22, p 241.
(12) Infelta, P. P. *Chem. Phys. Lett.* **1979**, *61*, 88.
(13) Tachiya, M. *Chem. Phys. Lett.* **1975**, *33*, 289.
(14) Almgren, M. *Adv. Coll. Interface Sci.* **1992**, *41*, 9.
(15) Gehlen, M. H.; De Schryver, F. C. *Chem. Rev.* **1993**, *93*, 199.
(16) Malliaris, A.; Le Moigne, J.; Sturm, J.; Zana, R. *J. Phys. Chem.* **1985**, *89*, 2709.
(17) Infelta, P. P.; Grätzel, M.; Thomas, J. K. *J. Phys. Chem.* **1974**, *78*, 190.
(18) Gehlen, M. H. *Chem. Phys. Lett* **1993**, *212*, 362.
(19) Quina, F. H.; Nassar, P. M.; Bonilha, J. B. S.; Bales, B. L. *J. Phys. Chem.* **1995**, *99*, 17 028.
(20) Sasaki, T.; Hattori, M.; Sasaki, J.; Nukina, K. *Bull. Chem. Soc. Jap.* **1975**, *48*, 1397.
(21) Hall, D. G. *J. Chem. Soc., Faraday Trans. 1* **1981**, *77*, 1121.
(22) Dearden, L. V.; Woolley, E. M. *J. Phys. Chem.* **1987**, *91*, 4123.
(23) Baar, C.; Buchner, R.; Kunz, W. *J. Phys. Chem. B* **2001**, *105*, 2906.
(24) Bales, B. L. *Proceedings of Colloque Ampere*; Magnetic Resonance in Colloid and Interface Science. 2001, submitted.
(25) Schreier, S.; Polnaszek, C. F.; Smith, I. C. P. *Biochim. et Biophys. Acta* **1978**, *515*, 375.
(26) Bales, B. L. Inhomogeneously Broadened Spin-Label Spectra. In *Biological Magnetic Resonance*; Berliner, L. J., Reuben, J., Eds.; Plenum Publishing Corporation: New York, 1989; Vol. 8, p 77.
(27) Marsh, D. Experimental Methods in Spin-Label Spectral Analysis. In *Spin Labeling. Theory and Applications*; Plenum Publishing Corporation: New York, 1989; Vol. 8, p 255.
(28) Mukerjee, P.; Ramachandran, C.; Pyter, R. A. *J. Phys. Chem.* **1982**, *86*, 3189.
(29) Bales, B. L.; Howe, A. M.; Pitt, A. R.; Roe, J. A.; Griffiths, P. C. *J. Phys. Chem. B* **2000**, *104*, 264.
(30) Schwartz, R. N.; Peric, M.; Smith, S. A.; Bales, B. L. *J. Phys. Chem.* **1997**, *101*, 8735.
(31) Bales, B. L.; Shahin, A.; Lindblad, C.; Almgren, M. *J. Phys. Chem. B* **2000**, *104*, 256.
(32) Hayter, J. B.; Penfold, J. *Colloid Polym. Sci.* **1983**, *261*, 1022.
(33) Hartley, G. S. *Aqueous Solutions of Parrifin-Chain Salts*; Hermann and Cie: Paris, 1936.
(34) Halle, B.; Carlström, G. *J. Phys. Chem.* **1981**, *85*, 2142.
(35) Cabane, B.; Duplessix, R.; Zemb, T. *J. Physique* **1985**, *46*, 2161.
(36) Berr, S. S.; Caponetti, E.; Johnson, J. S., Jr.; Jones, R. R. M.; Magid, L. J. *J. Phys. Chem.* **1986**, *90*, 5766.
(37) Berr, S. S.; Coleman, M. J.; Jones, R. R. M.; Johnson, J. S., Jr. *J. Phys. Chem.* **1986**, *90*, 6492.
(38) Berr, S. S. *J. Phys. Chem.* **1987**, *91*, 4760.
(39) Berr, S. S.; Jones, R. M. *Langmuir* **1988**, *4*, 1247.
(40) Berr, S.; Jones, R. R. M.; Johnson, J. S., Jr. *J. Phys. Chem.* **1992**, *96*, 5611.
(41) Bendedouch, D.; Chen, S.; Koehler, W. C. *J. Phys. Chem.* **1983**, *87*, 153.
(42) Lindman, B.; Wennerström, H.; Gustavsson, H.; Kamenka, N.; Brun, B. *Pure Appl. Chem.* **1980**, *52*, 1307.
(43) Tanford, C. *The Hydrophobic Effect: Formation of Micelles and Biological Membrane*, 2nd ed.; Wiley-Interscience: New York, 1980.
(44) Triolo, R.; Caponetti, E.; Graziano, V. *J. Phys. Chem.* **1985**, *89*, 5743.
(45) Yalkowsky, S. H.; Zografi, G. *J. Pharma. Sci.* **1972**, *61*, 793.
(46) Jones, L. L.; Schwartz, R. N. *Mol. Phys.* **1981**, *43*, 527.
(47) Bales, B. L.; Stenland, C. *J. Phys. Chem.* **1993**, *97*, 3418.
(48) Wikander, G.; Johansson, L. B.-Å. *Langmuir* **1989**, *5*, 728.
(49) Debye, P. *Trans. Electrochem. Soc.* **1942**, *82*, 265.
(50) Bales, B. L. *J. Phys. Chem. B* **2001**, *105*, 6798.
(51) Chaimovich, H.; Aleixo, R. M. V.; Cuccovia, I. M.; Zanette, D.; Quina, F. H. In *Solution Behavior of Surfactants*; Mittal, L. B., Fendler, L. B., Eds.; Plenum Press: New York, 1982; Vol. 2, p 949.
(52) Bunton, C. A.; Nome, F.; Quina, F. H.; Romsted, L. S. *Acc. Chem. Res.* **1991**, *24*, 357.
(53) Jönsson, B.; Lindman, B.; Holmberg, K.; Kronberg, B. *Surfactants and Polymers in Aqueous Solution*; John Wiley: Chichester, 1998.
(54) Ranganathan, R.; Tran, L.; Bales, B. L. *J. Phys. Chem.* **2000**, *104*, 2260.
(55) Ranganathan, R.; Peric, M.; Bales, B. L. *J. Phys. Chem.* **1998**, *102*, 8436.
(56) Ranganathan, R.; Okano, L. T.; Yihwa, C.; Quina, F. H. *J. Colloid Interface Sci.* **1999**, *214*, 238.
(57) Hoyer, H. W. *J. Phys. Chem.* **1957**, *61*, 1283.
(58) Barry, B. W.; Russell, G. F. J. *J. Colloid Interface Sci.* **1972**, *40*, 174.
(59) Anacker, E. W.; Rush, R. M.; Johnson, J. S. *J. Phys. Chem.* **1964**, *68*, 81.
(60) Thalberg, K.; van Stam, J.; Lindblad, C.; Almgren, M.; Lindman, B. *J. Phys. Chem.* **1991**, *95*, 8975.
(61) Roelants, E.; De Schryver, F. C. *Langmuir* **1987**, *3*, 209.
(62) Reekmans, S.; Luo, H.; Van der Auweraer, M.; De Schryver, F. C. *Langmuir* **1990**, *6*, 628.
(63) Corrin, M. L.; Harkins, W. D. *J. Am. Chem. Soc.* **1947**, *69*, 683.
(64) Gaillon, L.; Gaboriaud, R. *J. Chim. Phys.* **1997**, *94*, 728.
(65) Gaillon, L.; Hamidi, M.; Lelièvre, J.; Gaboriaud, R. *J. Chim. Phys.* **1997**, *94*, 707.
(66) Barry, B. W.; Wilson, R. *Colloid Polym. Sci.* **1978**, *256*, 251.
(67) Zana, R. *J. Colloid Interface Sci.* **1980**, *78*, 330.
(68) Courchene, W. L. *J. Phys. Chem.* **1964**, *68*, 1870.
(69) Mukerjee, P. *J. Colloid. Sci.* **1964**, *19*, 722.
(70) Tokiwa, F.; Ohki, K. *J. Phys. Chem.* **1967**, *71*, 1343.
(71) Evans, H. C. *J. Chem. Soc.* **1956**, 579.
(72) *Handbook of Chemistry and Physics*, 31st ed.; Chemical Rubber Publishing C.: Clevland, 1949.
(73) Zana, R. *J. Phys. Chem. B* **1999**, *103*, 9117.
(74) Gruen, D. W. R. *J. Colloid Interface Sci.* **1981**, *84*, 281.
(75) MacKerell, A. D., Jr. *J. Phys. Chem.* **1995**, *99*, 1846.
(76) Güveli, D. E.; Kayes, J. B.; Davis, S. S. *J. Colloid Interface Sci.* **1979**, *72*, 130.
(77) Tabony, J. *Mol. Phys.* **1984**, *51*, 975.
(78) Zana, R.; Lévy, H.; Papoutsi, D.; Beinert, G. *Langmuir* **1995**, *11*, 3694.
(79) Güveli, D. E.; Kayes, J. B.; Davis, S. S. *J. Colloid Interface Sci.* **1981**, *82*, 307.
(80) Mukerjee, P.; Mysels, K. J. *Critical Micelle Concentrations of Aqueous Surfactant Systems*; National Bureau of Standards: 1971.
(81) Emerson, M. F.; Holtzer, A. *J. Phys. Chem.* **1967**, *71*, 1898.
(82) Almgren, M.; Hansson, P.; Mukhtar, E.; van Stam, J. *Langmuir* **1992**, *8*, 2405.